J Solid State Electrochem (2015) 19:31–35
DOI 10.1007/s10008-014-2495-y

ORIGINAL PAPER

One-step preparation of the $BiVO_4$ film photoelectrode

Lucia H. Mascaro · Adam Pockett · John M. Mitchels · Laurence M. Peter · Petra J. Cameron · Veronica Celorrio · David J. Fermin · Jagdeep S. Sagu · K. G. Upul Wijayantha · Gabriele Kociok-Köhn · Frank Marken

Received: 10 February 2014 / Revised: 24 April 2014 / Accepted: 27 April 2014 / Published online: 22 May 2014

Abstract A one-step method of preparing photoelectrochemically active nanostructured $BiVO_4$ films is reported based on thermolysis (500 °C in air) of a polyethylene glycol (PEG300) "paint-on" precursor solution containing Bi^{3+} (as nitrate) and VO_4^{3-} (as the metavanadate ammonium salt). Films are formed directly on tin-doped indium oxide (ITO) substrates and characterised by electron microscopy (scanning electron microscopy (SEM), energy-dispersive X-ray spectroscopy (EDS)), X-ray diffraction, Raman spectroscopy, and photoelectrochemistry. The nanocrystalline film exhibited typically up to 52 % incident photon to current efficiency (IPCE) at 1.0 V vs. saturated calomel electrode (SCE) in aqueous 0.5 M Na_2SO_4 with oxalate, strongly enhancing photocurrents.

Keywords Water splitting · Photoanode · Oxygen evolution · Solar energy · Vanadium oxide · Nanostructure

L. H. Mascaro · A. Pockett · J. M. Mitchels · L. M. Peter · P. J. Cameron · G. Kociok-Köhn · F. Marken (✉)
Department of Chemistry, University of Bath, Bath BA2 7AY, UK
e-mail: F.Marken@bath.ac.uk

L. H. Mascaro
Department of Chemistry, San Carlos Federal University, Rod. Washington Luiz, km 235, CEP 13565-905 São Carlos, SP, Brazil

V. Celorrio · D. J. Fermin
School of Chemistry, University of Bristol, Bristol, Avon BS8 1TS, England

J. S. Sagu · K. G. U. Wijayantha
Department of Chemistry, University of Loughborough, Loughborough, Leicestershire LE11 3TU, England

Introduction

Bismuth vanadate ($BiVO_4$) is an n-type semiconductor, which is usually used as a yellow pigment, but which has recently also attracted attention for use in photoelectrochemical water splitting [1–4] and in the photolytic destruction of organic pollutants [5, 6]. The advantages offered by $BiVO_4$ are (i) a suitable band gap (usually 2.4 to 2.5 eV for monoclinic $BiVO_4$; however, a wider range of values has been reported), (ii) inexpensive components, and (iii) excellent stability in aqueous media, making this material a promising photoanode for visible light harvesting. More recent studies have focused on the preparation of $BiVO_4$, seeking to improve photocatalytic activity by using various strategies such as morphology control, construction of nanocomposite structures, and doping. $BiVO_4$ can be fabricated by solution-based methods including aqueous, hydrothermal, and solvothermal processes [7–9] or by spray pyrolysis [10]. In most of the synthesis methods proposed in the literature, several hours of reflux and use of aggressive chemicals such as concentrated nitric acid are required. In addition, often $BiVO_4$ is obtained as powder material, and when it is employed in photoelectrodes, an extra preparation step (conversion of powder to thin film) is necessary. For example, an elegant solvothermal method using an ethylene glycol–water–sodium oleate system was proposed by Wang et al., where the precursor solution was treated in a Teflon-lined autoclave at 180 °C for 24 h and $BiVO_4$ powder was produced [11]. Sayama et al. used a modified method of metal-organic decomposition and a polyethylene glycol solvent followed by evaporation under vacuum to obtain $BiVO_4$ films on tin-doped indium oxide (ITO) [12]. In this paper, we propose a relatively simple and direct one-step route to photoactive $BiVO_4$ nanostructured films based on combining $Bi(NO_3)_3$ and NH_4VO_3 directly in polyethylene glycol (PEG300) as solvent and applying this

precursor solution to ITO-coated glass, followed by thermal treatment at 500 °C in air.

Experimental

Reagents used were $Bi(NO_3)_3 \cdot 5H_2O$, NH_4VO_3, polyethylene glycol (PEG300), and Na_2SO_4 from Sigma-Aldrich (UK). Aqueous solutions were prepared with deionised and filtered water taken from a Thermo Scientific water purification system (Barnstead Nanopure, UK). Electrochemical measurements were performed with a μAutolab Type II potentiostat system (Ecochemie, Utrecht, Netherlands) with Autolab GPES software.

A solar simulator Xe lamp with 100 mW cm^{-2} (AM1.5) output was employed in cyclic voltammetry photoelectrochemical experiments. In some experiments, a high-power blue LED (λ=405 nm, M405L2 UV LED, Thorlabs, Ely, UK) together with LED driver (T-Cube LED driver, Thorlabs, Ely, UK) and a DDS Function/Arbitrary TG4001 Generator (TTi, Huntingdon, UK) were employed. The electrode/electrolyte contact area was 1 cm^2, front-lit, and the electrolyte was 0.5 M Na_2SO_4. Field emission scanning electron microscopy (FE-SEM) images were obtained using a JEOL JSM6301F microscope. Photocurrent spectra (incident photon to current efficiency (IPCE) data) were plotted as a function of incident light with λ ranging from 350 to 550 nm in steps of 10 nm. Light intensity of this optical window was calibrated using a standard silicon photodiode. The light chopping frequency was set at 0.5 Hz to minimise the attenuation affects. The apparatus was based on a Stanford Research Systems SR830 (Stanford, USA) lock-in amplifier, SR540 chopper controller, a home-made potentiostat, a 75-W xenon lamp powered by a Bentham 650 (Reading, UK) power supply, and a monochromator controller PMC3B of Bentham Instruments Ltd. (Reading, UK). Raman spectroscopy studies were carried out with an inVia Renishaw Raman microscope system (Gloucestershire, UK). The crystal phase of the $BiVO_4$ thin film was confirmed by X-ray diffraction (XRD, Bruker AXS D8 Advance diffractometer with a θ–2θ configuration and using CuKα radiation λ=1.5418 Å). Diffuse reflectance spectra were obtained using a UV–vis–NIR spectrometer (PerkinElmer Lambda 35).

The electrodes used were a platinum wire counter electrode and a potassium chloride saturated calomel (SCE) reference electrode. The working electrodes were made from glass coated with ITO (Image Optics Components, Basildon, Essex, UK), cut to give 1 cm×3 cm electrodes (sonicated at 30 min in acetone, washed with distilled water, and heated for 1 h at 500 °C before use).

For $BiVO_4$ film production, initially two solutions were prepared. The first solution was prepared by dissolving 1.036 g of $Bi(NO_3)_3 \cdot 5H_2O$ in 5 mL of PEG300 and the second by dissolving 0.25 g of NH_4VO_3 in 5 mL of PEG300. The solutions were then mixed to form a dark orange solution, which was agitated in an ultrasonic bath for 30 min. This mixture was then used as the precursor for deposition of $BiVO_4$ films. The deposition was carried out by employing a drawing roller (hard rubber lino printing roller) [13]. The precursor solution was distributed evenly onto the ITO substrate (ca. 20 μL cm^{-2} to give an average thickness of 0.2 to 0.5 μm), and it was then pre-dried with warm air for 15 min. The process was repeated to increase the thickness of the film. After this deposition, the coated ITO was heated at 500 °C (this temperature was chosen to give high-quality $BiVO_4$ films without deformation of the underlying glass slide) for 1 h in a tube furnace in the presence of air. The ITO glass film substrate was fully covered with a yellow adherent film after the preparation process.

Results and discussion

The Raman spectrum and XRD data for $BiVO_4$ thin films are shown in panels a and b of Fig. 1, respectively. From the Raman data, it is possible to observe characteristic peaks at around 210, 324, 368, 720, and 828 cm^{-1}, corresponding to the Raman active vibrational modes consistent with a pure monoclinic phase film of $BiVO_4$ [14]. The appearance of V-O band at 828 cm^{-1} indicates good crystallinity [15, 16]. The broad peak at 1,100 cm^{-1} corresponds to the ITO substrate. Figure 1b shows the XRD pattern for the $BiVO_4$ film sample. The indexed peaks are associated mainly with the planes of the monoclinic $BiVO_4$ structure (PDF No. 01-083-1699). The characteristic strong peak of tetragonal zircon phase at 24° was not observed, and therefore, there is no tetragonal zircon-type $BiVO_4$ phase present in the samples [17]. It is also possible to observe further diffraction peaks from the underlying ITO substrate, identified with an asterisk symbol in Fig. 1b. A scanning electron micrograph (SEM) of a $BiVO_4$ film is shown in Fig. 1c, where agglomeration of individual crystallites is observed. The SEM image shows that the film is dense, crystalline, and with particles typically around 1 to 2 μm in diameter. The energy-dispersive X-ray spectroscopy (EDS) data analysis in Fig. 1d revealed the presence of the elements Bi, V, and O in the film with approximately 1:1 atomic ratio for Bi:V.

Typical cyclic voltammograms for the $BiVO_4$ film on ITO in aqueous 0.5 M Na_2SO_4 solution in light and in the dark are shown in Fig. 2a. Two characteristic redox systems centred at approximately −0.1 V (weak) and at −0.4 V vs. SCE (strong) are indicative of reduction and re-oxidation of two different types of V^{5+} to V^{4+} surface states (tentatively assigned; or possibly also accumulation of charges in the conduction band, which has been reported to have mixed V, Bi, and O character [18, 7]). An anodic photocurrent is observed commencing

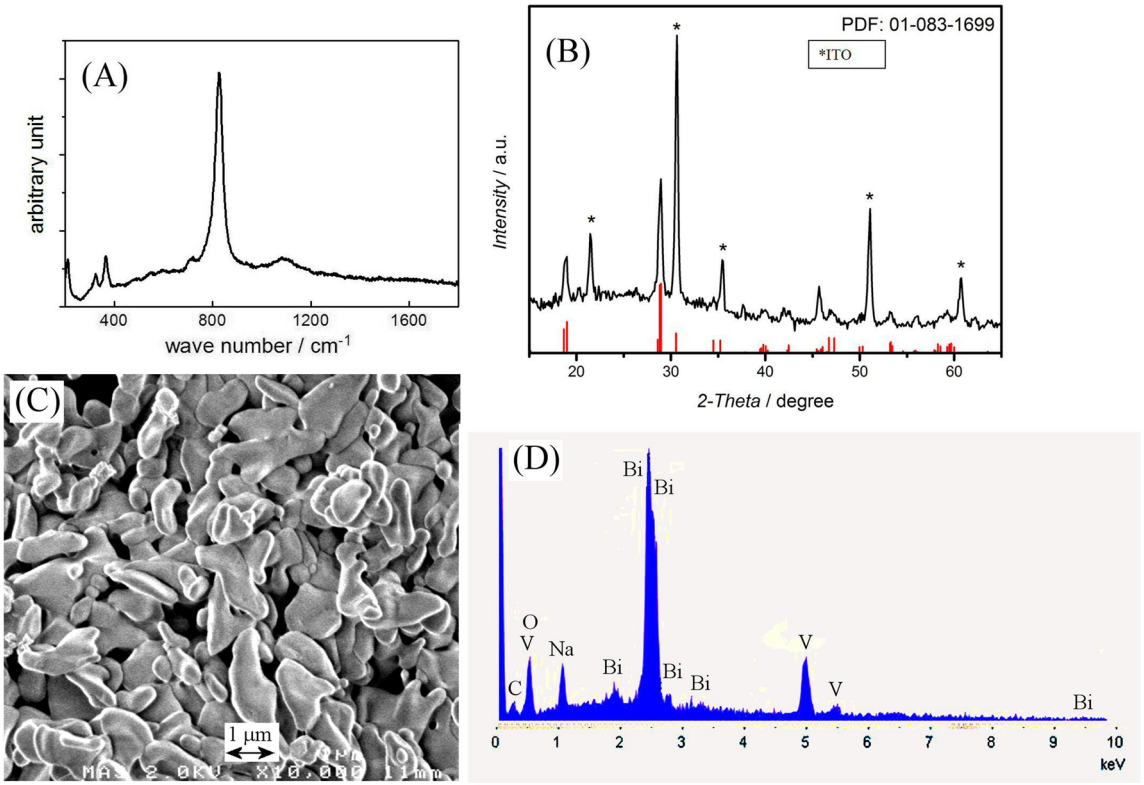

Fig. 1 **a** Raman spectrum, **b** X-ray diffraction pattern, and **c** FE-SEM image with **d** EDS analysis for the $BiVO_4$ thin film electrode formed on ITO

from ca. 0.0 V vs. SCE, which increases with increased bias potential when under illumination. The anodic photocurrent is associated with photooxidation of water. Hysteresis in the photocurrent profile is likely to be linked to local pH changes within the porous film structure. At 1.0 V vs. SCE, a typical value for the photocurrent is 300 μA cm^{-2} under solar simulator conditions (AM1.5). Substantially lower photocurrents were reported for example by Chatchai et al. using FTO/SnO_2/$BiVO_4$ and FTO/$BiVO_4$ film photoanodes [19]. The photocurrent observed in this work is larger than most results reported in the literature for pure $BiVO_4$ films [19–21] and consistent with high-quality films with good electrical contact to the underlying substrate.

The diffuse reflectance spectra of the samples were measured (see Fig. 2b). The band gap can be estimated as 2.52 eV (see red line), which is close to the values reported previously [10, 11, 13, 17]. In contrast, tetragonal zircon-type $BiVO_4$ has been reported to exhibit a wider less beneficial band gap (2.9 eV) [18]. Therefore, the results are consistent with Raman and XRD data, which indicate the presence of only the monoclinic $BiVO_4$ phase. In Fig. 2c, the IPCE values for $BiVO_4$/ITO electrodes are presented as a function of the irradiation wavelength measured at +1.0 V vs. SCE anodic bias in 0.5 M Na_2SO_4 solution. The electrodes show photocurrent responses in the visible light region up to about 490 nm (see inset), in accordance with the literature. Again, a band gap of approximately 2.52 eV (see red line), characteristic of $BiVO_4$, is observed. The ITO/$BiVO_4$ electrode shows a high efficiency for solar light conversion in both regions of UV and visible light. The maximum value of IPCE was 52 %, which is considerable when compared to typical results reported in the literature [19–23] but lower than the 73 % IPCE data (at 420 nm) reported by Jie et al. [24].

Both this study and that by Jie et al. [24] are based on a thermolysis process involving a precursor solution, which may have beneficial effects on the resulting substrate to $BiVO_4$ film interface. This interface is crucial in allowing effective flow of electrons into the underlying ITO substrate as well as in minimising recombination by oxygen reacting with V (IV) or directly at the ITO surface. The nature of this interface is likely to be affected by the gradual evaporation of PEG and residual components forming during thermolysis.

The presence of recombination processes can be demonstrated by addition of an oxalate hole quencher into the aqueous phase and study of photocurrents under pulsed blue light conditions. Figure 3 shows data for (a) a $BiVO_4$ electrode immersed in 0.5 M Na_2SO_4 and (b) the same experiment in the presence of 8 mM oxalate and (c) in the presence of 50 mM oxalate (all at pH 5). In the absence of oxalate, a typical light pulse transient response is observed with crossover from anodic to cathodic photocurrent pulse depending on the scan direction. This behaviour suggests non-steady-state behaviour possibly due to pH gradients developing in the solution close to the electrode surface. With 8 mM oxalate present (Fig. 3b),

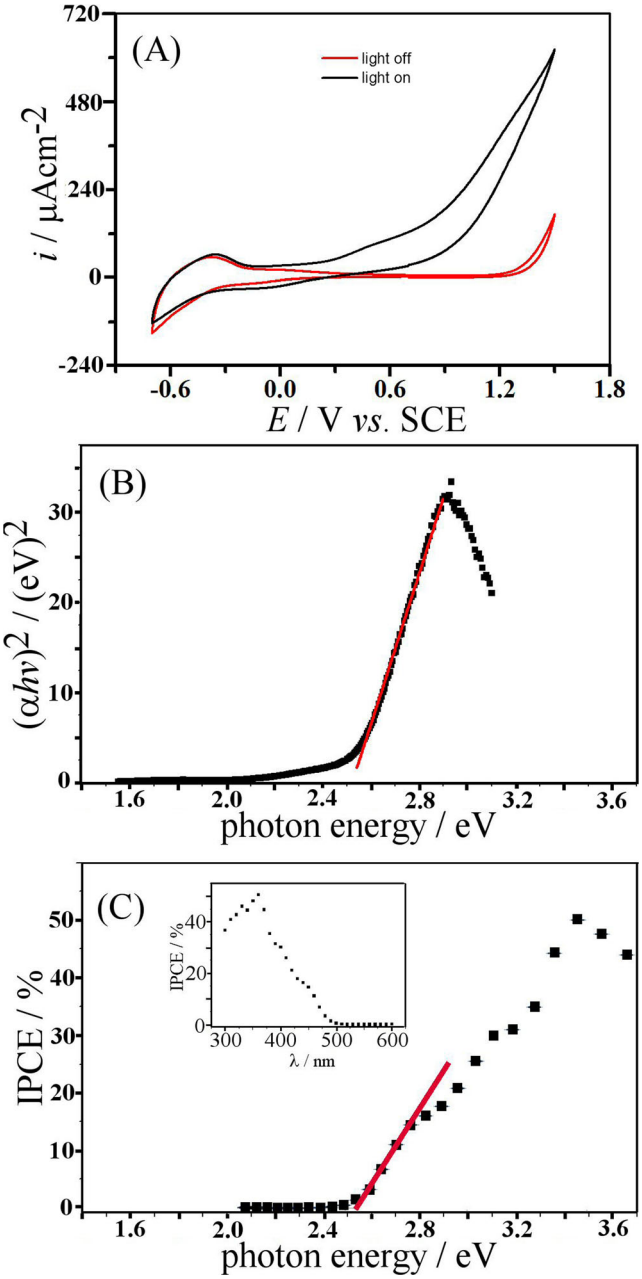

Fig. 2 **a** Cyclic voltammetry (scan rate 20 mVs^{-1}) for a $BiVO_4$ film electrode in 0.5 M Na_2SO_4 in the dark and light (AM1.5 solar simulator, 100 mW cm^{-2} Xe lamp). **b** Diffuse reflectance data plot $(\alpha h\nu)^2$ vs. photon energy for a $BiVO_4$ thin film on ITO. **c** IPCE plot for a $BiVO_4$ thin film at 1.0 V vs. SCE in 0.5 M Na_2SO_4. *Inset*: IPCE plot vs. wavelength

features are similar but now significantly higher photocurrents are detected. Oxalate is able to react with two holes from the photoexcited $BiVO_4$ to give CO_2 [25] (this is possible even on the ITO substrate [26], but the process is believed to be dominated here by $BiVO_4$). Therefore, recombination via solution processes can be suppressed. Further increase in oxalate concentration to 50 mM (see Fig. 3c) causes only minor further enhancement. There are two distinct steps in

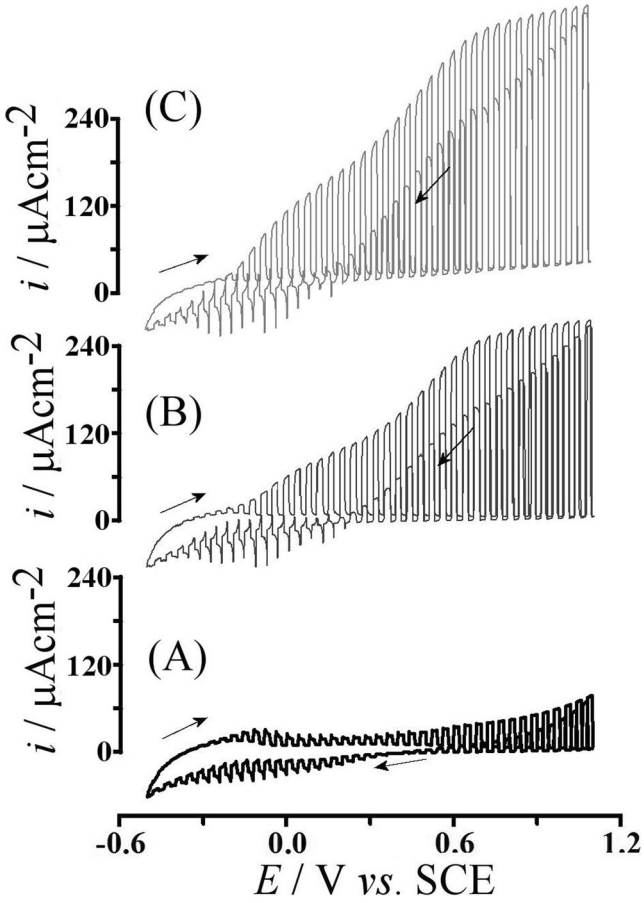

Fig. 3 **a**–**c** Cyclic voltammetry (scan rate 20 mVs^{-1}) for a $BiVO_4$ film electrode in 0.5 M Na_2SO_4 **a** with 8 mM oxalate **b** and with 50 mM oxalate **c** in the presence of pulsed light (blue LED, 0.5 Hz)

the photocurrent possibly due to the increase in applied bias potential causing a change in reaction pathway. Even higher concentrations of oxalate were observed to gradually corrode $BiVO_4$ (presumably by extraction of Bi^{3+} cations) associated with an increase in the dark current.

Conclusions

A crystalline, homogeneous, and adherent $BiVO_4$ thin film with monoclinic structure was produced on ITO substrate electrodes using a one-step method based on a PEG300 precursor solution. The method is experimentally simple, fast, and inexpensive and leads to an effective ITO–$BiVO_4$ interface. The photoanode material obtained exhibits photocurrents over a large potential range and with good IPCE values. It can be concluded that the "paint-on" synthesis of $BiVO_4$ films presented in this work is promising for use as photoelectrodes in water splitting, in photocatalytic degradation of organics, or in dye-sensitised solar cells [27]. Work on a wider range of substrates and applications is in progress.

Acknowledgments LHM thanks FAPESP (proc. 2012/23422-5). VC gratefully acknowledges the UK National Academy for support through the Newton International Fellows program. We thank the EPSRC for funding (DTC studentship for Adam Pockett, Grant EP/G03768X/1).

References

1. Ding C, Shi J, Wang D, Wang Z, Wang N, Liu G, Xiong F, Li C (2013) Phys Chem Chem Phys 15:4589–4595
2. Saito R, Miseki Y, Sayama K (2013) J Photochem Photobio A: Chem 258:51–60
3. Pilli SK, Deutsch TG, Furtak TE, Brown LD, Turner JA, Herring AM (2013) Phys Chem Chem Phys 15:3273–3278
4. Jeong HW, Jeon TH, Jang JS, Choi W, Park H (2013) J Phys Chem C 117:9104–9112
5. Shi W, Yan Y, Yan X (2013) Chem Engineer J 215:740–746
6. da Silva MR, Dall'Antonia LH, Scalvi LVA, dos Santos DI, Ruggiero LO, Urbano A (2012) J Solid State Electrochem 16:3267–3274
7. Park Y, McDonald KJ, Choi KS (2013) Chem Soc Rev 42:2321–2337
8. Zhang J, Luo W, Li W, Zhao X, Xue G, Yu T, Zhang C, Xiao M, Li Z, Zou Z (2012) Electrochem Commun 22:49–52
9. Myung N, Ham S, Choi S, Chae Y, Kim WG, Jeon YJ, Paeng KJ, Chanmanee W, de Tacconi NR, Rajeshwar K (2011) J Phys Chem C 115:7793–7800
10. Li MT, Zhao L, Guo L (2010) Int J Hydrogen Energy 35:7127–7133
11. Wang X, Li G, Ding J, Peng H, Chen K (2012) Mater Res Bull 47: 3814–3818
12. Sayama K, Nomura A, Zou Z, Abe R, Abe Y, Arakawa H (2003) Chem Commun 2908–2909.
13. Ahmed S, Hassan IAI, Roy H, Marken F (2013) J Phys Chem C 117: 7005–7012
14. Frost RL, Henry DA, Weier ML, Martens W (2006) J Raman Spectroscopy 37:722–732
15. Yao MM, Liu MX, Gan LH, Zhao FQ, Fan XZ, Zhu DZ, Xu ZJ, Hao ZX, Chen LW (2013) Coll Surf A-Physicochem Engineer Aspects 433:132–138
16. Kho YK, Teoh WY, Iwase A, Mädler L, Kudo A, Amal R (2011) Appl Mater Interfaces 3:1997–2004
17. Luo W, Wang Z, Wan L, Li Z, Yu T, Zou Z (2010) J Phys D Appl Phys 43:405402
18. Walsh A, Yan Y, Huda MN, Al-Jassim MM, Wei SH (2009) Chem Mater 21:547–551
19. Chatchai P, Murakami Y, Kishioka SY, Nosaka AY, Nosaka Y (2008) Electrochem Solid State Lett 11:H160–H163
20. Abdi FF, Firet N, van de Krol R (2013) ChemCatChem 5:490–496
21. Nagabhushana GP, Nagaraju G, Chandrappa GT (2013) J Mater Chem A 1:388–394
22. Liu H, Nakamura R, Nakato Y (2005) J Electrochem Soc 152:G856–G861
23. Zhou M, Bao J, Bi W, Zeng Y, Zhu R, Tao M, Xie Y (2012) Chem Sus Chem 5:1420–1425
24. Jia QX, Iwashina K, Kudo A (2012) PNAS 109:11564–11569
25. Byrne JA, Eggins BR (1998) J Electroanal Chem 457:61–72
26. Tansil NC, Xie H, Gao ZQ (2004) J Phys Chem B 108:16850–16854
27. Dong W, Guo YP, Guo B, Li H, Liu HZ, Joel TW (2013) ACS Appl Mater Interfaces 5:6925–6929